

WEIGHTED ENUMERATION OF NONBACKTRACKING WALKS ON WEIGHTED GRAPHS *

FRANCESCA ARRIGO[†], DESMOND J. HIGHAM[‡], VANNI NOFERINI[§], AND RYAN
WOOD[¶]

Abstract. We extend the notion of nonbacktracking walks from unweighted graphs to graphs whose edges have a nonnegative weight. Here the weight associated with a walk is taken to be the product over the weights along the individual edges. We give two ways to compute the associated generating function, and corresponding node centrality measures. One method works directly on the original graph and one uses a line graph construction followed by a projection. The first method is more efficient, but the second has the advantage of extending naturally to time-evolving graphs. Based on these generating functions, we define and study corresponding centrality measures. Illustrative computational results are also provided.

Key words. Complex network, matrix function, generating function, line graph, combinatorics, evolving graph, temporal network, centrality measure, Katz centrality.

MSC codes. 05C50, 05C82, 68R10

1. Introduction. Complex network analysis is an expanding scientific discipline that has recently been producing many research challenges, with applications across several fields of science and engineering [11, 24]. One important question is that of ranking the nodes of a graph by importance, or, in more mathematical terms, defining and studying an appropriate *centrality measure*. Those centrality measures that can be formulated and computed via combinatorial properties of walks on the underlying graph have received special attention [7, 12, 13, 19, 23] because they have convenient formulations in terms of linear algebra that lead to efficient computational methods. In recent years, this paradigm has been refined by studying centrality measures that are based on counting not all walks but only some of them, namely, walks that do not backtrack [1, 2, 5, 14, 28–30] or more generally do not cycle [5]. Nonbacktracking walks are known to be linked to zeta functions of graphs [18, 21, 22, 26]. Their associated centrality measures have been shown to possess attractive computational properties [1, 2, 4, 14] and have been studied both for undirected and directed graphs, and more recently for time evolving graphs [3]. However, in the context of the combinatorics of nonbacktracking walks, so far only unweighted graphs have been studied. We mention that nonbacktracking random walks were previously considered in [20], but the problems studied there are different to the ones analyzed in the present paper. Moreover, [20] focuses only on the special case where the nodes are given themselves a positive weight $\varphi(i)$, and the weight of the edge (i, j) is defined as $\omega((i, j)) = \varphi(i)\varphi(j)$.

*Submitted to the editors DATE.

[†]Department of Mathematics and Statistics, University of Strathclyde, Glasgow, UK, G1 1XH (francesca.arrigo@strath.ac.uk). The work of F.A. was supported by fellowship ECF-2018-453 from the Leverhulme Trust.

[‡]School of Mathematics, University of Edinburgh, James Clerk Maxwell Building, Edinburgh, UK, EH9 3FD (d.j.higham@ed.ac.uk). The work of D.J.H. was supported the Engineering and Physical Sciences Research Council under grants EP/P020720/1 and EP/V015605/1.

[§]Aalto University, Department of Mathematics and Systems Analysis, P.O. Box 11100, FI-00076, Aalto, Finland (vanni.noferini@aalto.fi). S supported by a n A cademy o f F inland g rant (Suomen Akatemian päätös 331230).

[¶]Corresponding author. Aalto University, Department of Mathematics and Systems Analysis, P.O. Box 11100, FI-00076, Aalto, Finland (ryan.wood@aalto.fi). S supported by a n A cademy o f F inland grant (Suomen Akatemian päätös 331240)

36 Instead, we do not impose any restriction on the edges' weights. In the theory of graph
 37 zeta functions, weighted graphs have been considered by defining the weight of a walk
 38 to be the sum (and not the product, as in this paper) of the weights of its edges [18].
 39 We discuss this issue further in section 2.

40 The main purpose of the present paper is to extend the combinatorial theory of
 41 nonbacktracking walks, and corresponding centrality measures, to graphs whose edges
 42 carry a positive *weight*. These graphs are associated with generic nonnegative adja-
 43 cency matrices, in contrast to unweighted graphs that correspond to binary adjacency
 44 matrices. While for unweighted graphs one may be interested in the enumeration of
 45 walks of a given length, for weighted graphs the combinatorial problem is more so-
 46 phisticated due to the presence of weights. The edge weights naturally give rise to
 47 an overall weight for each walk, a concept that can be used alongside the length (i.e.,
 48 the number of edges traversed).

49 The structure of the paper is as follows. In Section 2 we introduce some relevant
 50 notation and core concepts. Section 3 sets up and studies the issue of characterizing
 51 the classical generating function associated with nonbacktracking weighted walks and
 52 using it to compute a centrality measure. In section 4 we introduce an alternative
 53 formulation that applies to a wider class of generating functions and centrality mea-
 54 sures. Section 5 shows how these ideas can be extended to the case of evolving graphs.
 55 Numerical experiments are conducted in Section 6. We finish in Section 7 with a brief
 56 discussion.

57 **2. Background and Notation.** In this paper, we consider finite graphs. A
 58 finite graph is a triple $G = (V, E, \Omega)$ where $V = [n]$ is the set of the nodes (or
 59 vertices), $E \subset V \times V$ is the set of (directed) edges, and $\Omega : E \rightarrow (0, \infty)$ is a weight
 60 function that associates to each edge a positive weight. If $\Omega(e) = 1$ for all $e \in E$,
 61 then the graph is said to be *unweighted*; if for any pair $i \neq j$, with $i, j \in V$ we have
 62 that $(i, j) \in E \Leftrightarrow (j, i) \in E$ and that $\Omega((i, j)) = \Omega((j, i))$ then the graph is said to be
 63 *undirected*; and if, for every $i \in V$, we have that $(i, i) \notin E$ then the graph is said to be
 64 without loops. Graphs that are not unweighted are usually called *weighted* and graphs
 65 that are not undirected are usually called *directed*. It is, however, convenient (and
 66 we will do so within this work) to relax the terminology so that the set of directed
 67 (resp., weighted) graphs contains as special cases also undirected (resp., unweighted)
 68 graphs, further we will assume that all graphs are without loops.

69 A *walk of length ℓ* on the graph G is a sequence of nodes $i_1, i_2, \dots, i_{\ell+1}$ such that
 70 $(i_j, i_{j+1}) \in E$ for all $1 \leq j \leq \ell$. Equivalently, it can be seen as a sequence of edges
 71 e_1, \dots, e_ℓ such that $e_j \in E$ for all $j = 1, \dots, \ell - 1$ and the end node of e_j coincides
 72 with the starting node of e_{j+1} .

73 **DEFINITION 2.1.** *Let $G = (V, E, \Omega)$ be a weighted graph. The weight of the walk*
 74 *e_1, \dots, e_ℓ is*

$$75 \quad \prod_{k=1}^{\ell} \Omega(e_k)$$

76 *where $\Omega(e_k)$ is the weight of the edge $e_k \in E$.*

77 **REMARK 2.2.** *When $\Omega : E \rightarrow \{1\}$ is the weight function associated with an un-*
 78 *weighted graph, then the weight of all walks in the network is one, regardless of their*
 79 *length.*

80 In the context of mainstream graph theory, the *weight* (or *length* or *cost*) of a walk is
 81 sometimes defined as the *sum*, rather than the *product*, of the weights of its edges. In

82 that scenario, zeta functions of graphs (which are closely related to the enumeration
 83 of nonbacktracking walks) have been studied [18]. However, we argue that within
 84 complex network analysis Definition 2.1 has several useful applications. For example,
 85 consider a road network where nodes represent towns and a nonnegative integer edge
 86 weight A_{ij} records the number of distinct roads connecting town i and town j . Then,
 87 the number of distinct routes from i to j that pass through one intermediate town is
 88 equal to

$$89 \quad \sum_{k=1}^n A_{ik} A_{kj},$$

90 that is, the weighted sum of walks of length two, where the weight is the *product* of the
 91 weights of its edges. Similarly, in a model where edges represent independent prob-
 92 abilistic events and their weights are their probabilities, as discussed in the original
 93 work of Katz [19], it is natural to postulate that the weight of a walk is the product
 94 of the weight of its edges, in agreement with the fact that the joint probability of a
 95 sequence of independent events is the product of the individual probabilities.

96 Given a node ordering, the corresponding adjacency matrix of a graph is the
 97 matrix $A \in \mathbb{R}^{n \times n}$ entrywise defined as:

$$98 \quad A_{ij} = \begin{cases} 0 & \text{if } (i, j) \notin E; \\ \Omega((i, j)) & \text{if } (i, j) \in E. \end{cases}$$

99 Note that a graph is undirected if and only if its adjacency matrix is symmetric;
 100 it is without loops if and only if its adjacency matrix has zero diagonal; and it is
 101 unweighted if and only if its adjacency matrix has entries all lying in $\{0, 1\}$.

102 The problems of enumerating walks in unweighted graphs and enumerating weighted
 103 walks in weighted graphs may both be solved by considering powers of the adjacency
 104 matrix: indeed, the (i, j) entry of A^k is equal to, respectively, the number of walks
 105 of length k from node i to node j (when the graph is unweighted) or the weighted
 106 sum of walks of length k from node i to node j (when the graph is weighted). As a
 107 consequence, the generating function for the (possibly weighted) enumeration of walks
 108 is given by

$$109 \quad I + tA + t^2 A^2 + \dots = \sum_{k=0}^{\infty} t^k A^k = (I - tA)^{-1},$$

110 where we adopt the standard convention that the (weighted) sum of walks of length
 111 zero from i to j is 1 if $i = j$ and 0 otherwise. Here, t is a real parameter small enough
 112 to ensure convergence of the series which scales by t^k the count for walks of length k .

113 A walk can also be seen as a sequence of nodes. If the sequence does not contain
 114 a subsequence of the form iji for some nodes i and j , then the walk is said to be
 115 *nonbacktracking* (NBT). We define $p_k(A)$ to be the matrix whose (i, j) entry contains
 116 the sum of the weights of all nonbacktracking walks of length k from node i to node j .
 117 By convention, $p_0(A) = I$. Note that, by definition, $p_k(A) \leq A^k$ elementwise. Combi-
 118 natorially, the problem of computing the (weighted) enumeration of nonbacktracking
 119 walks is equivalent to finding an explicit expression for the generating function

$$120 \quad (2.1) \quad \Phi(t) = \sum_{k=0}^{\infty} t^k p_k(A)$$

121 for suitable values of the parameter $t > 0$.

122 This problem was addressed in [14] for unweighted undirected graphs, and later
 123 in [1] for unweighted directed graphs. In [2], the solution was extended to the more
 124 general generating function

$$125 \quad (2.2) \quad \kappa(t) = \sum_{k=0}^{\infty} c_k t^k p_k(A),$$

126 where $(c_k)_k \subset [0, \infty)$ is an arbitrary sequence. In [3], the theory was further extended
 127 to consider time evolving graphs. However, so far, the quantities (2.1) and (2.2)
 128 have not yet been studied for weighted graphs. Their characterization is the main
 129 contribution of this paper.

130 A corollary of obtaining such computable expressions is a numerical recipe for
 131 associated nonbacktracking centralities. Indeed, beyond its algebraic interpretation
 132 as a generating function, (2.2) can be interpreted analytically as a function that will
 133 converge for sufficiently small values of the variable t . Choosing one such value for
 134 t allows us to define a centrality measure based on the weighted sum of edges. For
 135 example, if $\mathbf{1}$ is the vector of all ones, then the i -th component of the vector

$$136 \quad \left(\sum_{k=0}^{\infty} c_k t^k p_k(A) \right) \mathbf{1}$$

137 computes a nonbacktracking version of Katz centrality [19]. The latter is defined as
 138 the doubly weighted sum of all the walks departing from node i , where the weight of
 139 each walk within the sum is the product of the weight of the walk itself and t^k , where
 140 k is the walk length. Similarly, for the *subgraph centrality* version of nonbacktracking
 141 Katz, the doubly weighted sum of all the walks that start and end on node i is given
 142 by

$$143 \quad \left(\sum_{k=0}^{\infty} c_k t^k p_k(A) \right)_{ii}.$$

144 As a consequence, two additional questions that we address in this paper are to
 145 describe the radius of convergence of (2.2) and to derive computable expressions for
 146 the associated centrality measures. We refer to [1, 2, 14], and the references therein,
 147 for details of the benefits of nonbacktracking in the centrality context.

148 We consider two approaches to bridge the gap between weighted graphs and
 149 current results on the combinatorics of nonbacktracking walks. The first is specialized
 150 to the case $c_k \equiv 1$, i.e., to compute (2.1); it leads directly to an expression that has
 151 computational advantages as it does not require to go through the edge-level and,
 152 thus, it requires the construction of a potentially much smaller matrix than the second
 153 approach. The second is based on a technique, described in [3, 5], of forming the line
 154 graph, obtaining a generating function there, and finally projecting back to compute
 155 (2.2). While, potentially, the second approach may be computationally less efficient,
 156 it has the advantages that (i) it is able to solve the more general problem (2.2), (ii)
 157 it can be generalized to the setting of time evolving graphs, and (iii) it allows us to
 158 easily estimate the convergence radius of (2.2) (including the special case of (2.1)).

159 **3. The generating function of nonbacktracking walks on a weighted**
 160 **graph.** In this section, we assume that G is a finite directed weighted graph with n
 161 nodes, without loops, and having adjacency matrix A . The directed edge from node
 162 i to node j has weight $A_{ij} > 0$. Following Definition 2.1, to the walk $i_1 i_2 i_3 \dots i_{\ell+1}$

163 of length ℓ we assign the weight $A_{i_1 i_2} A_{i_2 i_3} \cdots A_{i_{\ell} i_{\ell+1}}$. We note the distinction here
 164 between the *length* and the *weight* of a walk.

165 The goal of this section is to obtain a convenient formula for the generating
 166 function $\Phi(t)$ in (2.1). We note that this generalizes the version previously studied
 167 for an unweighted graph [1], and the expression $\Phi(t)\mathbf{1}$ is then a natural candidate for
 168 a node centrality measure.

169 **3.1. Describing the matrices $p_k(A)$ via a recurrence relation.** Let us first
 170 set up some further notation: given two square matrices $X, Y \in \mathbb{R}^{n \times n}$ we distinguish
 171 between matrix multiplication, XY , and elementwise multiplication, $X \circ Y$, where
 172 $(X \circ Y)_{ij} = X_{ij} Y_{ij}$. Similarly, we differentiate between the k -th linear algebraic
 173 power X^k and the k -th elementwise power, $X^{\circ k}$, so $(X^{\circ k})_{ij} = (X_{ij})^k$. Moreover,
 174 following Matlab notation, $\text{dd}(X) := \text{diag}(\text{diag}(X))$ will denote the diagonal matrix
 175 whose diagonal entries are equal to the diagonal entries of X . We first prove the
 176 following k -term recurrence, which generalizes previous results that have been derived
 177 independently for the unweighted [10, 27] and undirected [26] cases.

178 **THEOREM 3.1.** *For all $k \geq 1$,*

$$179 \quad p_k(A) = \sum_{\substack{\ell=2h+1 \text{ odd} \\ 1 \leq \ell \leq k}} (A^{\circ(h+1)} \circ (A^T)^{\circ h}) p_{k-\ell}(A) - \sum_{\substack{\ell=2h \text{ even} \\ 2 \leq \ell \leq k}} \text{dd}((A^{\circ h})^2) p_{k-\ell}(A).$$

180 *Proof.* For the base case of $k = 1$, the statement reduces to $p_1(A) = (A \circ$
 181 $\mathbf{1}\mathbf{1}^T) p_0(A)$. Since $A \circ \mathbf{1}\mathbf{1}^T = A$ and $p_0(A) = I$, in turn this yields $p_1(A) = A$,
 182 which is manifestly true since any walk of length one is nonbacktracking. Let us now
 183 give a proof by induction.

184 We start by considering $A p_{k-1}(A)$, whose (i, j) entry is equal to the sum of the
 185 weights of all walks of length k from i to j that are nonbacktracking if the first step is
 186 removed. This value is equal to $p_k(A)_{ij}$ plus the sum of the weights of all backtracking
 187 walks of length k from i to j that are nonbacktracking if the first step is removed.
 188 Such walks must be of the form $iaia \dots j$: the weight of one such walk is $A_{ia} A_{ai}$ times
 189 the weight of a certain NBT walk of length $k - 2$ from i to j . Summing over all a
 190 adjacent to i yields $\text{dd}(A^2) p_{k-2}(A)$. However, we have subtracted too much, because
 191 any such walk of the form $iaia \dots j$, being backtracking after removing the first step,
 192 was not present in $(A p_{k-1}(A))_{ij}$. The weight of one such walk is $A_{ia} A_{ai} A_{ia} = A_{ia}^2 A_{ai}$
 193 times the weight of a certain NBT walk of length $k - 3$ from a to j . We can sum again
 194 over all a adjacent to i , to obtain $((A^{\circ 2} \circ A^T) p_{k-3}(A))_{ij}$. We should sum this value
 195 back, but again we are adding a bit too much, because walks satisfying the previous
 196 requirements and being of the form $iaiaia \dots j$ should not be there.

197 It is clear that this sequence of corrections goes on until we exhaust the length
 198 of the walk and the statement of the theorem is a consequence of the two following
 199 facts, both true for all $h \geq 0$.

- 200 1. The total weight of walks of length k from i to j of the form $i(ai)^h a \dots j$, such
 201 that the final subwalk (of length $k - (2h + 1)$) from a to j is not backtracking,
 202 is equal to

$$203 \quad \sum_{a:(i,a) \in E} (A_{ia})^{h+1} (A_{ai})^h p_{k-2h-1}(A)_{aj} = \left((A^{\circ(h+1)} \circ (A^T)^{\circ h}) p_{k-2h-1}(A) \right)_{ij}.$$

- 204 2. The total weight of walks of length k from i to j of the form $(ia)^{2h} i \dots j$, such
 205 that the final subwalk (of length $k - 2h$) from i to j is not backtracking, is

206 equal to

$$207 \sum_{a:(i,a) \in E} (A_{ia})^h (A_{ai})^h p_{k-2h}(A)_{ij} = (\text{dd}((A^{\circ h})^2) p_{k-2h-1}(A))_{ij}. \quad \square$$

208 **3.2. Solving the recurrence relation.** Let us continue by giving a combina-
 209 torial result in Proposition 3.2. Its statement expresses the generating function of a
 210 sequence satisfying a growing recurrence relation in terms of two individual generating
 211 functions.

212 **PROPOSITION 3.2.** *Let $(\mathcal{P}_k)_k$ and $(\mathcal{C}_\ell)_\ell$ be two sequences in some (possibly non-*
 213 *commutative) ring, and suppose that $(\mathcal{P}_k)_k$ satisfies the growing recurrence*

$$214 \sum_{\ell=0}^k \mathcal{C}_\ell \mathcal{P}_{k-\ell} = 0$$

215 *for all $k \geq 1$. Then, the (formal) generating functions $\Phi(t) = \sum_{k=0}^{\infty} \mathcal{P}_k t^k$ and $\Psi(t) =$*
 216 *$\sum_{\ell=0}^{\infty} \mathcal{C}_\ell t^\ell$ are related by the formula $\Psi(t)\Phi(t) = \mathcal{C}_0 \mathcal{P}_0$.*

217 *Proof.* Observe that, using the recurrence,

$$218 \Psi(t)\Phi(t) = \sum_{k=0}^{\infty} t^k \sum_{\ell=0}^{\infty} \mathcal{C}_\ell \mathcal{P}_{k-\ell} = \mathcal{C}_0 \mathcal{P}_0. \quad \square$$

219 We can now apply the general technique of Proposition 3.2 to the special case
 220 of the generating function (2.1), whose coefficients satisfy the recurrence described in
 221 Theorem 3.1. In other words, we specialize Proposition 3.2 to sequences in the ring
 222 $\mathbb{R}^{n \times n}$ where $\mathcal{P}_k = p_k(A)$ and

$$223 \mathcal{C}_\ell = \begin{cases} I & \text{if } \ell = 0; \\ -[A^{\circ(h+1)} \circ (A^T)^{\circ h}] & \text{if } \ell = 2h + 1; \\ \text{dd}((A^{\circ h})^2) & \text{if } \ell = 2h > 0. \end{cases}$$

224 In particular, $\mathcal{C}_0 = \mathcal{P}_0 = I$, and hence by Proposition 3.2 $\Phi(t) = \Psi(t)^{-1}$. In turn, we
 225 can write $\Psi(t) = \Psi_e(t) - \Psi_o(t)$ by splitting even and odd terms and by extracting the
 226 minus sign appearing in the odd terms of $(\mathcal{C}_\ell)_\ell$. It is easy to see that $\Psi_e(t)$ is diagonal
 227 while $\Psi_o(t)$ is the off-diagonal part of $\Psi(t)$, since we assume G to be without loops.
 228 Moreover,

$$229 (\Psi_o(t))_{ij} = \sum_{h=0}^{\infty} t^{2h+1} A_{ij}^{h+1} A_{ji}^h = \frac{t A_{ij}}{1 - t^2 A_{ij} A_{ji}}.$$

230 Similarly,

$$231 (\Psi_e(t))_{ii} = 1 + \sum_{h=1}^{\infty} t^{2h} \sum_{j=1}^n A_{ij}^h A_{ji}^h = 1 + \sum_{j=1}^n \frac{t^2 A_{ij} A_{ji}}{1 - t^2 A_{ij} A_{ji}}.$$

232 Let $S = A \circ A^T$, let $Q = S^{\circ 1/2}$, let

$$233 f_1(x) = \frac{x}{1-x}, \quad f_2(x) = \frac{x}{1+x},$$

234 and let $f_i(\circ tX)$ denote the *elementwise* application of f_i to the matrix tX , for $i = 1, 2$.
 235 Then, if we denote by $\circ /$ the elementwise application of $/$, we can write

$$236 \quad \Psi_e(t) = I + \text{dd}(f_1(\circ tQ)f_2(\circ tQ)), \quad \Psi_o(t) = tA \circ / (\mathbf{1}\mathbf{1}^T - t^2S)$$

237 and hence $\Psi(t) = I + \text{dd}(f_1(\circ tQ)f_2(\circ tQ)) - tA \circ / (\mathbf{1}\mathbf{1}^T - t^2S)$.

238 We can state this more formally as a theorem.

239 **THEOREM 3.3.** *In the notation above, for all values of t such that (2.1) converges,*
 240 *we have*

$$241 \quad (3.1) \quad \Phi(t) = (I + \text{dd}[f_1(\circ tQ)f_2(\circ tQ)] - tA \circ / (\mathbf{1}\mathbf{1}^T - t^2S))^{-1}.$$

242 As a sanity check, let us see what happens in three distinct interesting limiting
 243 cases that have been addressed previously in the literature.

244 • First, let us verify that in the limit of an unweighted graph we recover [1,
 245 equation (3.3)]. In this case, $(A_{ij})^h = A_{ij} \in \{0, 1\}$ for all $h \geq 1$. As a result,
 246 if $D = \text{dd}(A^2)$,

$$247 \quad (\Psi_e(t))_{ii} = 1 + \sum_{h=1}^{\infty} t^{2h} \sum_{j=1}^n A_{ij}A_{ji} = 1 + D_{ii} \frac{t^2}{1-t^2} \Rightarrow \Psi_e(t) = \frac{I - t^2I + t^2D}{1-t^2}$$

248 and

$$249 \quad (\Psi_o(t))_{ij} = tA_{ij} + \sum_{h=1}^{\infty} t^{2h+1} A_{ij}A_{ji} = tA_{ij} + \frac{t^3S_{ij}}{1-t^2} \Rightarrow \Psi_o(t) = \frac{tA - t^3(A-S)}{1-t^2}$$

250 which imply the known $\Phi(t) = (1-t^2)(I - tA + t^2(D-I) + t^3(A-S))^{-1}$
 251 from [1, Equation (3.3)].

252 • Next, let us observe that if no edge is reciprocated, that is, if there is no $(i, j) \in$
 253 E such that $(j, i) \in E$, then $S = Q = 0$. Hence, we recover the generating
 254 function associated with classical Katz centrality, i.e., $\Phi(t) = (I - tA)^{-1}$,
 255 which is consistent with the fact that every walk is nonbacktracking under
 256 this assumption.
 257 • Finally, if the graph is undirected then $S = A^{\circ 2}$ and $Q = A$. Hence, the
 258 formulae simplify to

$$259 \quad \Psi_e(t) = I + \text{dd}[f_1(\circ tA)f_2(\circ tA)], \quad \Psi_o(t) = tA \circ / (\mathbf{1}\mathbf{1}^T - t^2A^{\circ 2})$$

260 yielding in particular

$$261 \quad \Phi(t) = (I + \text{dd}[f_1(\circ tA)f_2(\circ tA)] - tA \circ / (\mathbf{1}\mathbf{1}^T - t^2A^{\circ 2}))^{-1}.$$

262 If we additionally assume that the graph is unweighted, we further reduce to
 263 $\Phi(t) = (1-t^2)(I - At + t^2(D-I))^{-1}$ in agreement with [14, Equation (5.3)].

264 We now briefly comment on the convergence of $\Phi(t) = \sum_k p_k(A)t^k$ to the right-
 265 hand-side of (3.1). Since the series converges to a rational function, its radius of
 266 convergence is equal to the smallest of its poles. One way to compute the radius is
 267 therefore via the eigenvalues of the rational function $\Psi(t) = \Phi(t)^{-1}$. A more straight-
 268 forward method (albeit possibly less efficient) to estimate the radius of convergence
 269 is available when computing $\Phi(t)$ with a different method. This is described in more

270 detail in Section 3 and, in particular, within Corollary 4.8. In spite of the some-
 271 what awkward notation, (3.1) is in fact quite straightforward to compute given A , by
 272 composing elementwise functions and matrix addition and multiplications.

273 We conclude this section by recalling that we can define a nonbacktracking version
 274 of Katz centrality on weighted graphs by summing the value of the generating function
 275 over all possible ending nodes, which can be expressed as the linear algebraic matrix-
 276 vector multiplication $\Phi(t)\mathbf{1}$.

277 The following corollary is then an immediate consequence of Theorem 3.1.

278 **COROLLARY 3.4.** *For all values of t such that (2.1) converges, consider the cen-*
 279 *trality measure where node i is assigned the value x_i according to $\mathbf{x} = \Phi(t)\mathbf{1}$. Then \mathbf{x}*
 280 *may be found by solving the linear system*

$$281 \quad (3.2) \quad (I + \text{dd}[f_1(\circ tQ)f_2(\circ tQ)] - tA \circ / (\mathbf{1}\mathbf{1}^T - t^2S))\mathbf{x} = \mathbf{1}.$$

282 Corollary 3.4 shows in particular that the centrality measure can be found without
 283 explicitly computing the inverse in (3.1). We can instead compute the vector of
 284 nonbacktracking centralities \mathbf{x} by solving the linear system (3.2). We note that the
 285 coefficient matrix in (3.2) is no less sparse than $I - tA$; hence the computational
 286 complexity of solving such a linear system is the same as for classical Katz centrality,
 287 and the task is feasible with standard tools for sparse linear systems for very large,
 288 sparse networks.

289 **4. Generating function by constructing the line graph and projecting**
 290 **back.** In this section, we derive an alternative computable expression for the gener-
 291 ating function $\Phi(t)$. Although generally this second method is less computationally
 292 efficient, it offers three main advantages: (i) it can be extended to nonbacktracking
 293 centrality measures other than Katz (for example, based the exponential rather than
 294 the resolvent); (ii) it allows for a simple characterization of the radius of convergence
 295 of the generating function; and (iii) it can be extended to time evolving graphs.

As before, we consider a finite weighted graph with n nodes. We also assume
 (directed) edges have been labelled from 1 to m in an arbitrary, but fixed, manner.
 We may then define the *source matrix* $L \in \mathbb{R}^{m \times n}$ and *target (or terminal) matrix*
 $R \in \mathbb{R}^{m \times n}$ as follows [31]:

$$L_{ej} = \begin{cases} 1 & \text{if edge } e \text{ starts from node } j \\ 0 & \text{otherwise} \end{cases} \quad R_{ej} = \begin{cases} 1 & \text{if edge } e \text{ ends on node } j \\ 0 & \text{otherwise.} \end{cases}$$

296 Moreover, we let Z be an $m \times m$ diagonal matrix such that $Z_{ee} = A_{ij}$, where (in the
 297 chosen labelling of the edges) the e -th edge is precisely (i, j) .¹ Then, we have the
 298 following relationship.

299 **PROPOSITION 4.1.** *We have $A = L^T Z R$.*

300 *Proof.* Since Z is diagonal, $(L^T Z R)_{ij} = \sum_{e=1}^m L_{ei} Z_{ee} R_{ej}$. But there is at most
 301 one value of e such that $L_{ei} R_{ej} \neq 0$, and that is precisely the value identifying the
 302 edge $i \rightarrow j$, if this is an edge of the graph. If such an edge does not exist then the
 303 summation yields 0, as desired. If such an edge exists, then, for that e , $Z_{ee} = A_{ij}$
 304 which concludes the proof. \square

305 Now let W be the weighted matrix of the dual graph (or line graph), i.e., the
 306 graph whose nodes correspond to the original (directed) edges, and whose edges are

¹For clarity, we will sometimes use the notation $i \rightarrow j$ to denote the edge $(i, j) \in E$.

307 pairs of edges from the original graph that can form a walk. The pair $(i \rightarrow j, j \rightarrow k)$
 308 represents a walk that has weight equal to the product of the original edge weights;
 309 that is, $A_{ij}A_{jk}$. These values are recorded in the entries of W , with $W_{ef} = A_{ij}A_{jk}$ if
 310 e is the label of edge $i \rightarrow j$ and f is the label of edge $j \rightarrow k$.

311 **THEOREM 4.2.** *We have $W = ZRL^T Z$.*

Proof. We proceed entrywise. Suppose for concreteness that edge e is $i \rightarrow j$ and edge f is $k \rightarrow \ell$, where $i \neq j, k \neq \ell$ are (possibly, but not necessarily, all distinct) nodes. Note for a start that $W_{ef} = A_{ij}A_{j\ell}$ if $j = k$ and $W_{ef} = 0$ if $j \neq k$. Now, since Z is diagonal,

$$(ZRL^T Z)_{ef} = Z_{ee}Z_{ff} \sum_{h=1}^n R_{eh}L_{fh} = A_{ij}A_{k\ell} \sum_{h=1}^n R_{eh}L_{fh}.$$

312 Suppose $j \neq k$; then there is no h such that $R_{eh}L_{fh} \neq 0$, so the summation above is
 313 $0 = W_{ef}$. On the other hand, if $j = k$ then the summation over h yields 1 so that
 314 $(ZRL^T Z)_{ef} = A_{ij}A_{j\ell} = W_{ef}$. \square

315 In the unweighted case, we have a projection relation $L^T W^k R = A^{k+1}$ [5, Propo-
 316 sition 2.4]. However, for weighted graphs, entries of W^k count walks of length $k + 1$,
 317 but with incorrect weights. For example, the walk $1 \rightarrow 2 \rightarrow 3 \rightarrow 4$ would be weighted
 318 $A_{12}A_{23}^2A_{34}$ rather than $A_{12}A_{23}A_{34}$. We now exhibit a trick that corrects this prob-
 319 lem. Coherently with the notation of the previous section, below $M^{\circ 1/2}$ denotes the
 320 elementwise nonnegative square root of a nonnegative matrix M ; note that generally
 321 this does not correspond to the classical matrix square root \sqrt{M} (i.e., the matrix X
 322 such that $X^2 = M$), a notable exception being the case of a diagonal square matrix
 323 with nonnegative diagonal. We note that Z falls in this latter category, hence the
 324 notation in the following result.

325 **THEOREM 4.3.** *Let $0 < k \in \mathbb{N}$. The (e, f) element of $\sqrt{Z}(W^{\circ 1/2})^k \sqrt{Z}$ counts,
 326 with weights, all walks of length $k + 1$ from edge e to edge f .*

Proof. The crucial observation is that $W^{\circ 1/2} = \sqrt{Z}RL^T \sqrt{Z}$, which is clear by a minor modification of the proof of Theorem 4.2. We now proceed by induction on k . For the base case $k = 1$, it suffices to observe that $\sqrt{Z}W^{\circ 1/2}\sqrt{Z} = ZRL^T Z = W$. Suppose now that the statement holds for $k - 1$. Then,

$$\sqrt{Z}(W^{\circ 1/2})^k \sqrt{Z} = \sqrt{Z}(W^{\circ 1/2})^{k-1} \sqrt{Z}(Z^{-1/2})W^{\circ 1/2} \sqrt{Z}.$$

Define for notational simplicity $U := \sqrt{Z}(W^{\circ 1/2})^{k-1} \sqrt{Z}$, $X := Z^{-1/2}$, $Y := W^{\circ 1/2}$, $\Sigma := \sqrt{Z}$. Then, since X and Σ are diagonal,

$$(UXY\Sigma)_{ef} = \sum_{g \in E} U_{eg}X_{gg}Y_{gf}\Sigma_{ff}.$$

Suppose now that edge e is $i \rightarrow j$ and edge f is $h \rightarrow \ell$; then edges g must be of the form $x \rightarrow h$ for some node x . Indeed, $Y_{gf} = 0$ unless the end node of edge g coincides with the start node of edge f , i.e., unless gf is a walk of length two. Hence, in this notation,

$$(UXY\Sigma)_{ef} = \sum_{x:A_{xh}>0} U_{e,x \rightarrow h} \sqrt{A_{h\ell}A_{xh}} \sqrt{\frac{A_{h\ell}}{A_{xh}}} = A_{h\ell} \sum_{x:A_{xh}>0} U_{e,x \rightarrow h},$$

327 where $\sum_{x:A_{xh}>0} U_{e,x \rightarrow h}$ is, by the inductive assumption, the count (with weights) of
 328 all walks of length $k - 1$ from edge e to all edges of the form $x \rightarrow h$, i.e., the weighted
 329 enumeration of all walks of length $k - 1$ from edge e to node h . However, the count
 330 with weights of all walks of length k from edge e to edge f is precisely the count with
 331 weights of all walks of length k from edge e to node ℓ with node h as the penultimate
 332 node, i.e., the right hand side in the latter displayed equation. \square

333 We have the following consequence of Theorem 4.3.

334 COROLLARY 4.4. *For all $k \in \mathbb{N}$, $L^T \sqrt{Z}(W^{\circ 1/2})^k \sqrt{Z}R = A^{k+1}$.*

335 *Proof.* The result follows from Proposition 4.1, if $k = 0$, and from Theorem 4.3,
 336 if $k > 0$. \square

337 Now let $B \in \mathbb{R}^{m \times m}$ be the nonbacktracking version of W , i.e., $B_{ef} = 0$ if
 338 $W_{ef}W_{fe} \neq 0$ and $B_{ef} = W_{ef}$ otherwise. This matrix is often referred to as the
 339 *Hashimoto matrix* [16]. Recall, moreover, that $p_k(A) \in \mathbb{R}^{n \times n}$ is the matrix counting
 340 all NBT walks of length k (from i to j in its (i, j) element). Now we can observe that
 341 all the proofs above hold for B as well, modulo substituting walks with nonbacktrack-
 342 ing walks. Hence, the projection relation still holds.

343 THEOREM 4.5. *For all $k \in \mathbb{N}$, we have $L^T \sqrt{Z}(B^{\circ 1/2})^k \sqrt{Z}R = p_{k+1}(A)$.*

344 *Proof.* We have $p_1(A) = A = L^T ZR$, and when $k > 0$ the result follows from a
 345 minor modification of the arguments used to prove Corollary 4.4. \square

Suppose now that $(c_k)_k \subset [0, \infty)$ is a sequence and t is such that

$$\kappa(t, A) = \sum_{k=0}^{\infty} c_k t^k p_k(A)$$

346 as in (2.2) converges; we are interested in the centrality measure

$$347 \quad (4.1) \quad \mathbf{v}(t, A) = \kappa(t, A)\mathbf{1}.$$

We now derive formulae for $\kappa(t, A)$ and $\mathbf{v}(t, A)$. To this end, we introduce the following
 notation. Given a real-analytic scalar function

$$f(x) = \sum_{k=0}^{\infty} c_k x^k$$

consider the operator

$$\partial f(x) = \sum_{k=0}^{\infty} c_{k+1} x^k = \frac{f(x) - c_0}{x}.$$

348 We then have the following.

349 THEOREM 4.6. *It holds that*

$$350 \quad \sum_{k=0}^{\infty} c_k t^k p_k(A) = c_0 I + tL^T \sqrt{Z} \partial f(tV) \sqrt{Z}R,$$

351 for $V = B^{\circ 1/2}$ and $|t| < r/\rho(V)$, where $\rho(V)$ is the spectral radius of V and r is the
 352 radius of convergence of the scalar function $f(x) = \sum_{k=0}^{\infty} c_k x^k$.

Hence, for the centrality associated with $f(x)$ and t small enough to give conver-
 gence in the matrix power series, in (4.1) we have

$$\mathbf{v}(t, A) = c_0 \mathbf{1} + tL^T \sqrt{Z} \partial f(tV) \sqrt{Z} \mathbf{1}.$$

Proof. By Theorem 4.5 we easily see that

$$\kappa(t, A) = c_0 I + tL^T \sqrt{Z} \left(\sum_{k=0}^{\infty} c_{k+1} t^k (B^{\circ 1/2})^k \right) \sqrt{Z} R.$$

As a consequence,

$$\mathbf{v}(t, A) = c_0 \mathbf{1} + tL^T \sqrt{Z} \left(\sum_{k=0}^{\infty} c_{k+1} t^k (B^{\circ 1/2})^k \right) \sqrt{Z} \mathbf{1}.$$

353 Observing that the resolvent is an eigenfunction (with eigenvalue 1) of ∂ , we note
 354 in particular that for Katz centrality, i.e., $c_k = 1$ for all k , $\partial f(x) = f(x) = (1-x)^{-1}$.
 355 Hence, we have the following special case.

356 COROLLARY 4.7. *In the notation of Theorem 4.6, we have that the generating*
 357 *function $\Phi(t)$ defined in (2.1) can be expressed as*

$$358 \quad (4.2) \quad \Phi(t) = I + tL^T \sqrt{Z} (I - tV)^{-1} \sqrt{Z} R.$$

359 This analysis in particular yields a lower bound for the radius of convergence for
 360 (2.1).

361 COROLLARY 4.8. *If $|t| < \rho(V)^{-1}$, where $V = B^{\circ 1/2}$, then the sequence $\Phi(t) =$*
 362 *$\sum_{k=0}^{\infty} p_k(A) t^k$ converges.*

363 REMARK 4.9. *Letting r denote the radius of convergence of (2.1), Corollary 4.8*
 364 *shows that $r \geq \rho(V)^{-1}$. It is possible to strengthen this result and prove that $r =$*
 365 *$\rho(V)^{-1}$. A proof of this fact, which is beyond the scope of the present article, appears*
 366 *in [25, Theorem 5.2].*

367 **5. Nonbacktracking centralities for evolving weighted graphs.** In Sec-
 368 tions 3 and 4, we obtained formulae for the generating function $\Phi(t)$ in (2.1) by
 369 working, respectively, at node and edge level. For a static network, i.e., one which
 370 does not evolve in time, working at the node level is clearly preferable as, for large n ,
 371 we may have that $n \ll m$. However, a significant advantage of the latter, edge-level,
 372 formula is that it easily extends to the case of temporal networks in all backtracking
 373 regimes, whereas a direct node-level formula which forbids backtracking in time is
 374 generally unavailable [3]. Let us first generalize the definition of graph, walk, and
 375 NBT walk to the dynamic case.

376 DEFINITION 5.1. *A finite time-evolving graph \mathcal{G} is a finite collection of graphs*
 377 *$(G^{[1]}, \dots, G^{[N]})$, associated with the non-decreasing time stamps $(t_1, \dots, t_N) \in \mathbb{R}^N$,*
 378 *such that the set of nodes of $G^{[i]}$ does not depend on i and when observed at time t_i*
 379 *the structure of \mathcal{G} is identical to that of $G^{[i]}$.*

380 We remark that the concept of a graph can be extended to the dynamic setting in
 381 a number of ways [17]. The discrete-time framework of Definition 5.1 covers a range
 382 of realistic scenarios where interactions take place, or are recorded, at specific points
 383 in time. For example, in an on-line social media platform, an edge may represent a
 384 form of communication between users, and $G^{[i]}$ may count the number of interactions
 385 between each pair of individuals over time $(t_{i-1}, t_i]$.

386 The definition of walk across a network can be extended to the setting of temporal
 387 graphs as follows.

388 DEFINITION 5.2. A walk of length ℓ across a temporal network is defined as an
 389 ordered sequence of ℓ edges $e_1 e_2 \dots e_\ell$ such that for all $k = 1, \dots, \ell - 1$ the end node of
 390 e_k coincides with the start node of e_{k+1} and, moreover, that $e_k \in E^{[\tau_1]}, e_{k+1} \in E^{[\tau_2]}$
 391 for some $1 \leq \tau_1 \leq \tau_2 \leq N$, where $E^{[\tau_i]}$ denotes the set of edges of the graph $G^{[\tau_i]}$.

392 It is useful to make an equivalent definition.

393 DEFINITION 5.3. A walk of length ℓ across a temporal network is defined as an
 394 ordered sequence of $\ell + 1$ nodes $i_1 i_2 \dots i_{\ell+1}$ such that for all $k = 2, \dots, \ell$ it holds that
 395 $i_{k-1} \rightarrow i_k \in E^{[\tau_1]}$ and $i_k \rightarrow i_{k+1} \in E^{[\tau_2]}$ for some $1 \leq \tau_1 \leq \tau_2 \leq N$.

396 We want to stress that multiple edges can be crossed at one given time stamp and,
 397 moreover, that a walk is allowed to remain inactive for some of the time stamps.
 398 We also recall here that there is not just one definition of backtracking for temporal
 399 networks; indeed, three arise naturally [3]:

- 400 • backtracking happens within a certain time-stamp; we will refer to this as
 401 *backtracking in space*,
- 402 • backtracking happens across time-stamps; we will refer to this as *backtracking*
 403 *in time*,
- 404 • backtracking happens both within a time-stamp and across time-stamps (not
 405 necessarily in this order); we will refer to this as *backtracking in time and*
 406 *space*.

407 Given any finite time-evolving graph \mathcal{G} , we can associate with it a matrix M called
 408 the *global temporal transition matrix* which was defined in [3] for unweighted graphs.
 409 Definition 5.4 below generalizes the definition of the global temporal transition matrix
 410 to the weighted case.

411 DEFINITION 5.4. Let $\mathcal{G} = (G^{[1]}, G^{[2]}, \dots, G^{[N]})$ be a time-evolving graph with N
 412 time stamps. The weighted global temporal transition matrix associated with \mathcal{G} is the
 413 $m \times m$ block matrix

$$414 \quad (5.1) \quad M = M^{[1, \dots, N]} = \begin{bmatrix} C^{[1]} & C^{[1,2]} & C^{[1,3]} & \dots & C^{[1,N]} \\ 0 & C^{[2]} & C^{[2,3]} & \dots & C^{[2,N]} \\ \vdots & & \ddots & & \vdots \\ \vdots & & & \ddots & \vdots \\ 0 & \dots & \dots & 0 & C^{[N]} \end{bmatrix}^{\circ 1/2},$$

415 where the definition of the blocks depends on the chosen backtracking regime in the
 416 following way:

- 417 (i) $C^{[\tau_1]} = W^{[\tau_1]}$ and $C^{[\tau_1, \tau_2]} = W^{[\tau_1, \tau_2]} := S^{[\tau_1]} R^{[\tau_1]} (L^{[\tau_2]})^T S^{[\tau_2]}$ for all $\tau_1, \tau_2 =$
 418 $1, 2, \dots, N$ ($\tau_1 < \tau_2$) if backtracking in both space and time is permitted;
- 419 (ii) $C^{[\tau_1]} = B^{[\tau_1]}$ and $C^{[\tau_1, \tau_2]} = W^{[\tau_1, \tau_2]}$ for all $\tau_1, \tau_2 = 1, 2, \dots, N$ ($\tau_1 < \tau_2$) if
 420 backtracking in space is forbidden but backtracking in time is permitted;
- 421 (iii) $C^{[\tau_1]} = W^{[\tau_1]}$ and $C^{[\tau_1, \tau_2]} = B^{[\tau_1, \tau_2]} := W^{[\tau_1, \tau_2]} - (W^{[\tau_1, \tau_2]} \circ W^{[\tau_2, \tau_1]})^{\circ 1/2}$
 422 for all $\tau_1, \tau_2 = 1, 2, \dots, N$ ($\tau_1 < \tau_2$) if backtracking in time is forbidden but
 423 backtracking in space is permitted; and
- 424 (iv) $C^{[\tau_1]} = B^{[\tau_1]}$ and $C^{[\tau_1, \tau_2]} = B^{[\tau_1, \tau_2]}$ for all $\tau_1, \tau_2 = 1, 2, \dots, N$ ($\tau_1 < \tau_2$) if
 425 backtracking in both time and space is forbidden.

426 It was further shown in [3] that the global temporal transition matrix provides an
 427 accurate way of counting walks in all backtracking regimes across a finite unweighted
 428 time-evolving graph and thereby allows for the computation of the (nonbacktracking)

429 Katz centrality \mathbf{v} via the formula:

$$430 \quad (5.2) \quad \mathbf{v}(t) = (I + t\mathcal{L}^T(I - tM)^{-1}\mathcal{R})\mathbf{1},$$

431 where \mathcal{L}, \mathcal{R} are the global source and target matrices respectively as defined in [3,
432 Definition 4.4].

433 To handle the weighted case, we may extend Theorem 4.5 naturally to the global
434 temporal transition matrix M in the following way.

435 **THEOREM 5.5.** *For a finite time-evolving graph with N -many time frames, let the
436 global weight matrix Z be defined block-wise as*

$$437 \quad Z := Z^{[1,2,\dots,N]} = \text{diag}(Z^{[1]}, Z^{[2]}, \dots, Z^{[N]}),$$

438 where $Z^{[\tau_i]}$ is the diagonal matrix associated with time stamp $1 \leq \tau_i \leq N$. For each of
439 these matrices, their diagonal entries are given by $Z_{ee}^{[\tau_i]} = w_e^{[\tau_i]}$, with $w_e^{[\tau_i]}$ being the
440 weight of edge e at time stamp τ_i . Further let the backtracking regime be fixed such
441 that the weighted global temporal transition matrix M is fixed. Then, for $0 < k \in \mathbb{N}$,
442 the (e, f) -th entry of $\sqrt{Z}M^k\sqrt{Z}$ counts, with weights, all permitted walks of length
443 $k + 1$ from edge e to edge f across the time evolving graph given the backtracking
444 regime.

445 *Proof.* Suppose the backtracking regime is given such that the structure of M is
446 fixed as specified in Definition 5.4. We prove the theorem by induction on the length
447 of permitted walks $k \in \mathbb{N}$. Consider the basis case $k = 1$:

$$448 \quad \sqrt{Z}M\sqrt{Z} = \sqrt{Z} \begin{bmatrix} C^{[1]} & C^{[1,2]} & C^{[1,3]} & \dots & C^{[1,N]} \\ 0 & C^{[2]} & C^{[2,3]} & \dots & C^{[2,N]} \\ \vdots & & \ddots & & \vdots \\ \vdots & & & \ddots & \vdots \\ 0 & \dots & \dots & 0 & C^{[N]} \end{bmatrix}^{\circ 1/2} \sqrt{Z}.$$

449 The (e, f) -th element of this matrix correctly counts the unique walk of length
450 two with weights from edge e to edge f . In the following we will omit the temporal
451 superscript, since the indices e and f also uniquely determine the time frame. With
452 this convention:

$$453 \quad \left(\sqrt{Z}M\sqrt{Z}\right)_{ef} = \sum_{r,s} \sqrt{Z}_{er}M_{rs}\sqrt{Z}_{sf}$$

$$454 \quad = (\sqrt{Z})_{ee}(\sqrt{Z})_{ff}M_{ef}$$

$$455 \quad = \begin{cases} \sqrt{w_e}\sqrt{w_f}\sqrt{w_e w_f} = w_e w_f & ef \text{ is a permitted walk of length two} \\ 0 & \text{otherwise.} \end{cases}$$

$$456$$

457 where we have used the fact that, if ef is an admissible walk of length two, then
458 $(M)_{ef} = \sqrt{w_e w_f}$.

459 Suppose now that the result holds for $k-1$ and for brevity denote by P the matrix
460 $\sqrt{Z}M^{k-1}\sqrt{Z}$, which, by the inductive assumption, correctly counts in its entries the
461 number of weighted temporal walks of length k . Then, using the fact that Z is

462 diagonal,

$$\begin{aligned}
 463 \quad (\sqrt{Z}M^k\sqrt{Z})_{ef} &= \sum_{r,s,t} \left(\sqrt{Z}M^{k-1}\sqrt{Z} \right)_{er} (Z^{-1/2})_{rs} M_{st}(\sqrt{Z})_{tf} \\
 464 \quad &= \sum_r P_{er}(Z^{-1/2})_{rr} M_{rf}(\sqrt{Z})_{ff} \\
 465 \quad &= \begin{cases} w_f \sum_r P_{er} & e \dots rf \text{ is a permitted walk of length } k+1 \\ 0 & \text{otherwise.} \end{cases} \\
 466 \quad &
 \end{aligned}$$

467 By the inductive assumption P_{er} counts the permitted weighted walks of length
 468 k from edge e to edge r . Therefore the above formula does indeed count the weighted
 469 permitted walks beginning with edge e and ending on edge f with length $k+1$
 470 correctly. \square

471 **THEOREM 5.6.** *Given global source, target and weight matrices, \mathcal{L} , \mathcal{R} and Z re-*
 472 *spectively, we can compute M when backtracking is entirely forbidden in two steps:*

- 473 1. $\widehat{M} = \left(\sqrt{Z}(\mathcal{R}\mathcal{L}^T - \mathcal{R}\mathcal{L}^T \circ \mathcal{L}\mathcal{R}^T)\sqrt{Z} \right)$;
- 474 2. Obtain M from \widehat{M} by setting all entries below the block diagonal to 0.

475 *Proof.* The above theorem is easy to prove by observing that the (i, j) -th block of
 476 the matrix $\mathcal{R}\mathcal{L}^T$ is equal to $R^{[i]}L^{[j]T}$, whereas the (i, j) -th block of the matrix $\mathcal{L}\mathcal{R}^T$
 477 is equal to $L^{[i]}R^{[j]T} = (R^{[j]}L^{[i]T})^T$; whereupon the (i, j) -th block of the matrix \widehat{M}
 478 becomes

$$479 \quad \widehat{M}_{ij} = \sqrt{Z^{[i]}} \left(R^{[i]}L^{[j]T} - R^{[i]}L^{[j]T} \circ (R^{[j]}L^{[i]T})^T \right) \sqrt{Z^{[j]}}.$$

481 The central term here in brackets can be seen as the binarized $B^{[i,j]}$, i.e., $B^{[i,j]}$ where
 482 all non-zero weights are uniformly equal to 1, thus the presence of a non-zero entry
 483 $(B^{[i,j]})_{ef}$ simply reflects whether or not the concatenation of edges e and f forms a
 484 non-backtracking walk of length two. Matrix multiplication from the left by $\sqrt{Z^{[i]}}$
 485 and on the right by $\sqrt{Z^{[j]}}$ then provides the appropriate weighting for the (e, f) -th
 486 entry, namely $\sqrt{w_e}\sqrt{w_f}$, as required. Finally, the second step of setting all blocks
 487 below the block diagonal, i.e., \widehat{M}_{ij} with $i > j$, to zero reflects the requirement that
 488 walks may not move back in time. \square

489 We can also compute the f -total communicability of the time-evolving graph with
 490 weights by using the global temporal transition matrix M .

491 **THEOREM 5.7.** *Given a function f with series expansion $f(t) = \sum_{k=0}^{\infty} c_k t^k$ having*
 492 *radius of convergence r , and some fixed backtracking regime, the f -total communica-*
 493 *bility $\mathbf{v}_f(t)$ of the time-evolving graph $\mathcal{G} = (G^{[1]}, \dots, G^{[N]})$ with N time stamps is*
 494 *given by the formula:*

$$495 \quad (5.3) \quad \mathbf{v}_f(t) = (c_0 I + t \partial \mathcal{L}^T \sqrt{Z} f(tM) \sqrt{Z} \mathcal{R}) \mathbf{1}$$

496 for $0 < |t| < r / \max_{i=1, \dots, N} \{\rho(C^{[\tau_i]})\}$.

497 *Proof.* By Proposition 5.5, we have that $\sqrt{Z}M^k\sqrt{Z}$ counts with weights all walks
 498 of length $k+1$, thus

$$499 \quad \mathbf{v}_f(t) = (c_0 I + t \partial \mathcal{L}^T \sqrt{Z} f(tM) \sqrt{Z} \mathcal{R}) \mathbf{1} = c_0 I + t \sum_{k=0}^{\infty} c_{k+1} t^k \mathcal{L}^T \sqrt{Z} M^k \sqrt{Z} \mathcal{R} \mathbf{1}.$$

Table 6.1: Static network convergence information.

Non-binarized graph $\rho(B^{o1/2})$	926.9
Binarized graph $\rho(B)$	48.61
Non-binarized nonbacktracking permitted range of t	$t \in [0, 1.079 \cdot 10^{-3})$
Binarized nonbacktracking permitted range of t	$t \in [0, 2.057 \cdot 10^{-2})$
Non-binarized $\rho(A)$	1038
Binarized $\rho(A)$	51.26
Non-binarized backtracking permitted range of t	$t \in [0, 9.635 \cdot 10^{-4})$
Binarized backtracking permitted range of t	$t \in [0, 1.951 \cdot 10^{-2})$

500 In the above formula we see the number of walks of length $k + 1$ correctly counted
501 with weights that are further weighted by the coefficient $c_{k+1}t^{k+1}$, which is provided
502 by the series expansion of $f(x)$. \square

503 **6. Numerical Experiments.** In this section we show how the formulae for
504 nonbacktracking Katz centrality from sections 3, 4 and 5 may produce significantly
505 different node-rankings for real-world social networks when compared with Katz cen-
506 trality which permits backtracking walks. We further examine the effect of weighting
507 edges on the rankings produced by both centrality measures. To this end, we consider
508 the Katz centrality formula (5.2) as applied to one static network and one temporal
509 network, both derived from the same data set (Fauci’s email release [6])². The origi-
510 nal dataset is a collection of over 3000 pages of emails involving Anthony Fauci and his
511 staff during the COVID-19 pandemic. Data includes sender and receivers (including
512 CC’d) of emails, as well as time stamps of when the emails were sent. Both networks
513 used in the following were presented in [6].

514 **6.1. Analysis on Static Networks.** In this section, we analyze a static network
515 produced by [6] which is both undirected and weighted. We have an edge (i, j) if there
516 exists an email which involves both nodes i and j as any combination of sender and
517 recipient (including CC’d recipients). The weight assigned to such an edge, $\Omega((i, j))$,
518 is a positive integer equal to the number of such emails that were sent.

519 In our analysis, we apply Corollary 3.4 to obtain the NBT Katz centrality vector
520 for our network, which is then contrasted with the classical Katz centrality vector
521 for attenuation factor values $t = 0.5/\rho$ and $t = 0.95/\rho$, where $1/\rho$ is the radius of
522 convergence for the respective centrality measure. In particular $1/\rho$ is equal to $1/\rho(A)$,
523 where A is the adjacency matrix of the graph in the case of classical Katz centrality;
524 whereas $1/\rho = 1/\rho(B^{o1/2})$ in the case of weighted nonbacktracking Katz centrality [25,
525 Theorem 5.2], where B is the Hashimoto matrix associated to the graph. These values
526 are given in Table 6.1. We also analyze the binarized graph which is produced from
527 the static graph by setting all edge weights to 1. In the context of the binarized
528 network $1/\rho$ equals $1/\rho(A)$ in the case of classical Katz centrality, and $1/\rho(B)$ for
529 nonbacktracking Katz centrality, where A and B are the adjacency and Hashimoto
530 matrices associated with the binarized network, respectively.

531 The results are visualised in Figures 6.1, 6.2 and 6.3. Figure 6.1 shows that
532 NBT Katz centrality emphasizes a clique not containing the node corresponding to
533 Antony Fauci, and that for large values of the attenuation factor this clique begins to

²The code used in the following analysis can be found at <https://github.com/rwood12347/Weighted-enumeration-of-nonbacktracking-walks-on-weighted-graphs>

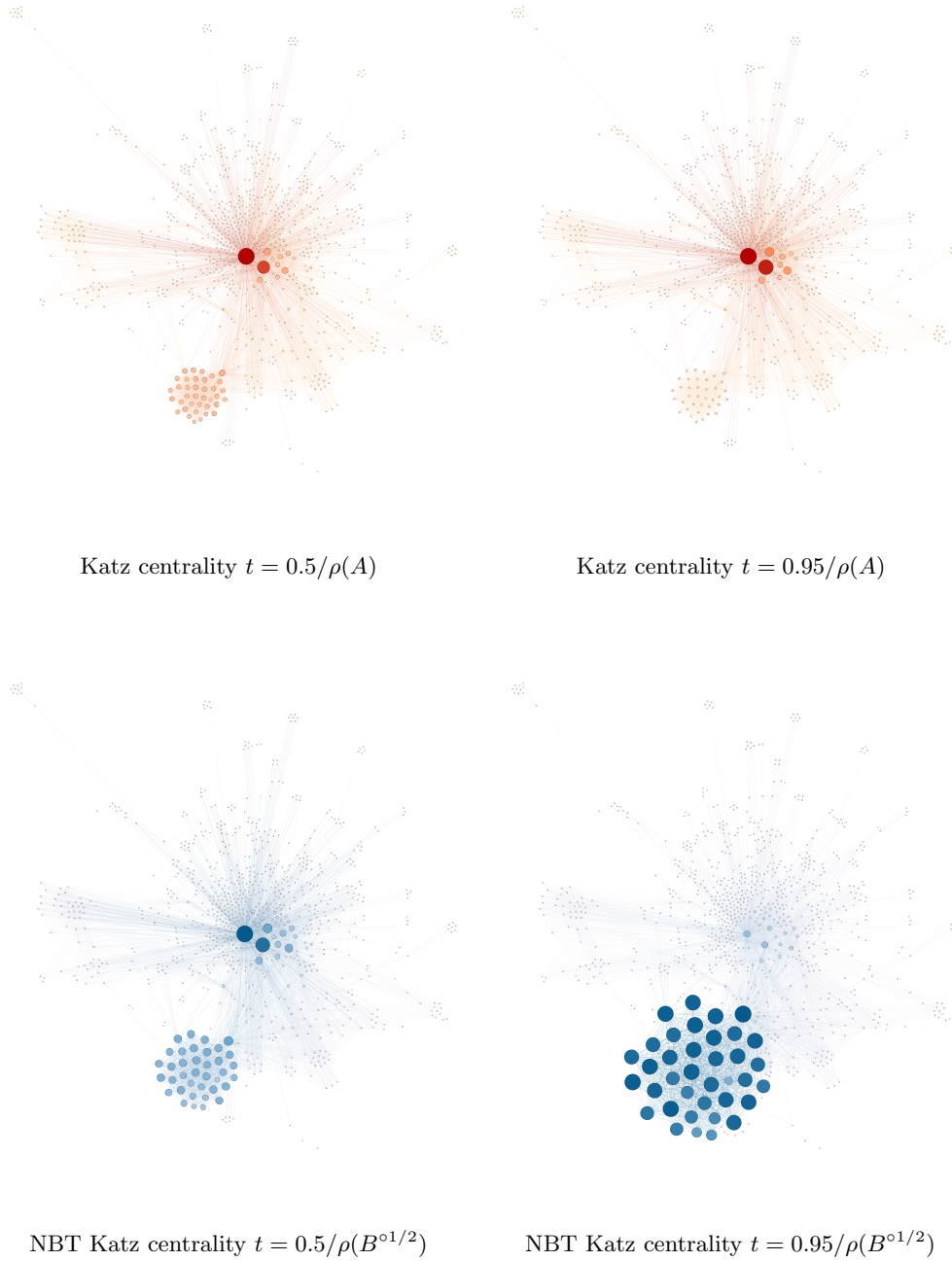


Fig. 6.1: Visualizations of classical (top/red) and NBT Katz (bottom/blue) across the static email network with large node size and dark colour indicating large centrality values; darker edges indicate a larger weight.

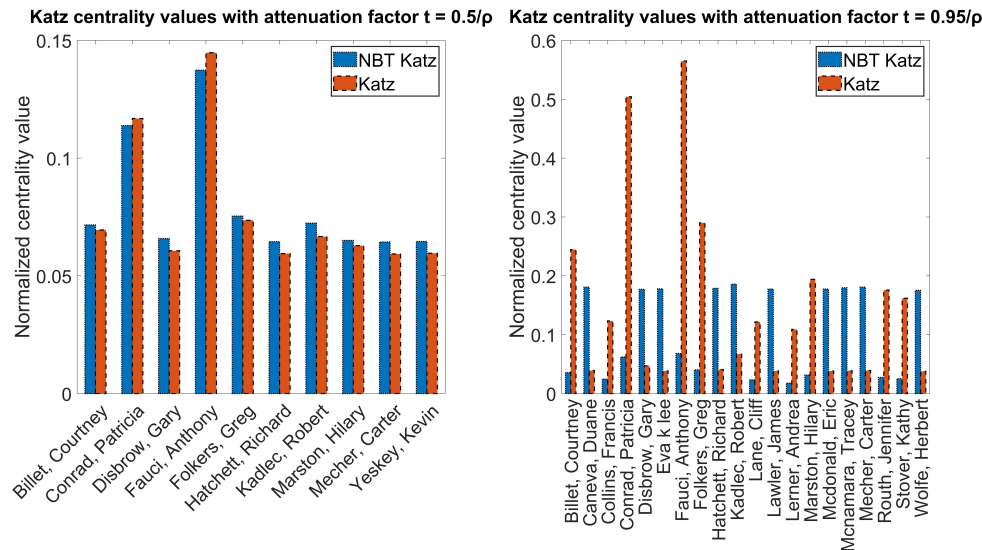


Fig. 6.2: Classical and nonbacktracking Katz centrality vector values for backtracking fully forbidden with attenuation factor $t = 0.5/\rho$ and $t = 0.95/\rho$, respectively. In each plot we display the union of the 10 most central nodes according to each centrality measure.

534 dominate the ranking to such an extent that the node corresponding to Anthony Fauci,
 535 which occupies the central position in the network visualisation, is no longer counted
 536 among the 10 most central nodes. This can be seen in Figure 6.2 which depicts the
 537 nonbacktracking and classical Katz normalized centrality values for the union of the
 538 10 most central nodes in the static network. The left bar chart in Figure 6.2 indicates
 539 that both classical and nonbacktracking Katz agree on the 10 most central nodes of
 540 which ‘Anthony Fauci’ is most central when $t = 0.5/\rho$. However the rightmost figure
 541 depicts a complete divergence in the ten most highly-ranked nodes produced by classic
 542 and nonbacktracking Katz centralities respectively. In particular we see that while
 543 the ‘Anthony Fauci’ node remains fairly central according to both measures, nodes
 544 belonging to the clique shown in Figure 6.1 have overtaken it in the ranking induced by
 545 nonbacktracking Katz centrality. The clique identified in this case consists exclusively
 546 of participants (i.e., either directly sent or received an email within the thread, or were
 547 CC’d in an email within the thread) in the so-called ‘Red Dawn’ email thread that
 548 was used throughout the pandemic “to provide thoughts, concerns, raise issues, share
 549 information across various colleagues responding to Covid-19” [8].

550 The effect of weighted edges on the rankings produced by nonbacktracking and
 551 classical Katz centralities for the static network is demonstrated in Figure 6.3. The
 552 figure contains two scatter graphs of the normalized nonbacktracking Katz centrality
 553 vector ($t = 0.95/\rho(B^{o1/2})$) plotted against the Katz centrality vector ($t = 0.95/\rho(A)$)
 554 for both the original network (right) and a binarized modified network (left), which
 555 is formed from the original network by setting all edge weights to 1.

556 In particular we see that the presence of non-uniformly weighted edges in the net-
 557 work produces greater variation in the nonbacktracking and classical Katz centrality
 558 vectors.

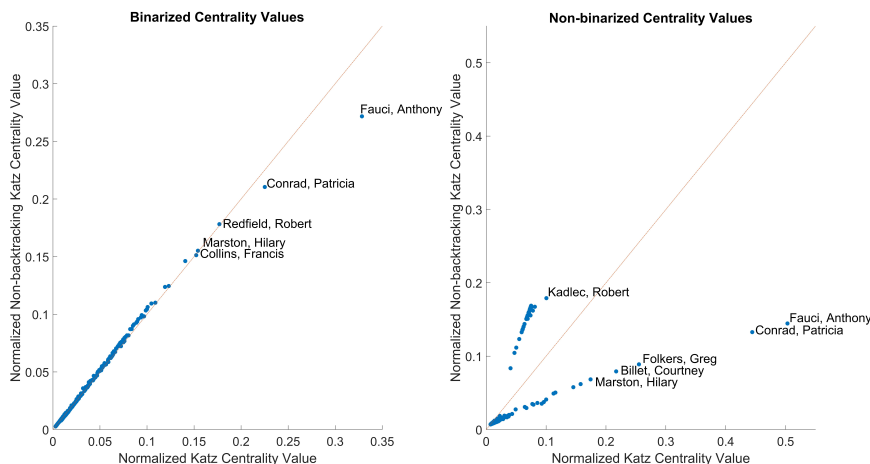


Fig. 6.3: Scatter plots of normalized NBT Katz centrality against normalized classical Katz centrality corresponding to binarized and non-binarized static networks with attenuation factor $t = 0.95/\rho$.

559 **6.2. Analysis on Temporal Networks.** We now move on to the case of a
 560 time-dependent network, and we note that the special case of an unweighted network
 561 with backtracking permitted corresponds to the work in [15] wherein the *dynamic*
 562 *communicability matrix* $\mathcal{Q}(t)$ associated to such a network is defined as the product
 563 of the successive resolvents

$$564 \quad (6.1) \quad \mathcal{Q}(t) = (I - tA^{[1]})^{-1}(I - tA^{[2]})^{-1} \dots (I - tA^{[N]})^{-1}.$$

565 Here $A^{[i]}$ is the adjacency matrix associated to the i -th time-stamp of the temporal
 566 network \mathcal{G} . Katz centrality can then be computed via the formula

$$567 \quad (6.2) \quad \mathbf{x}(t) = \mathcal{Q}(t)\mathbf{1}.$$

568 This formula accounts for all walks across the temporal network \mathcal{G} including those
 569 that backtrack in space and between time-stamps.

570 The temporal network \mathcal{G} analyzed in this section is the largest temporal strong
 571 component [9] of the provided email data, i.e., the largest component that is connected
 572 in the sense that there exists a time-respecting path between any two nodes contained
 573 within. This network consists of a collection of 100 directed networks associated with
 574 the date 2018-09-04 and the 99 consecutive days between 2020-01-26 and 2020-05-05.
 575 In this network we have a directed weighted edge $(i, j) \in E(G^{[T_t]})$, if node j is a
 576 recipient of, or is CC'd in, an email sent by node i . The weight of such an edge is
 577 equal to the number of such emails sent during the t -th timestamp.

578 We reiterate here that when treating temporal networks there is a range of possible
 579 nonbacktracking regimes, as outlined in Definition 5.4. The choice of appropriate
 580 backtracking regime is highly context-dependent. For the data set analyzed here, it
 581 is reasonable to forbid backtracking entirely, since the time-stamps associated with
 582 the temporal network have an almost uniform spacing of one day, and the time taken
 583 to reply to an email is on a similar scale to the spacing between time-stamps. It is

Table 6.2: Temporal network convergence information.

$\rho(M)$	5.025
nonbacktracking permitted range of t	$t \in [0, 0.1990)$
$\max_i(\rho(A^{[i]}))$	8.832
Backtracking permitted range of t	$t \in [0, 0.1132)$

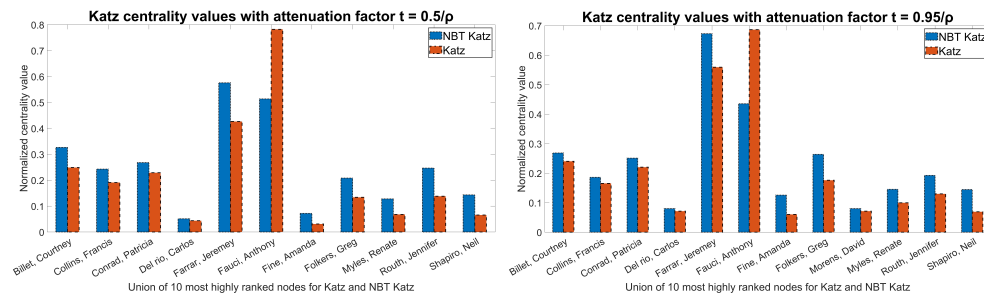


Fig. 6.4: The time-evolving network centrality vector values for both NBT and classical Katz with attenuation factor $t = 0.5/\rho$ and $t = 0.95/\rho$ respectively. In each plot we display the union of the ten most central nodes according to each centrality measure.

584 worth mentioning that this choice to fully forbid backtracking is subjective and other
 585 regimes may also be reasonable.

586 Our analysis of the spectrum of the global temporal transition matrix M associ-
 587 ated to the graph \mathcal{G} with backtracking fully-forbidden yields the permitted ranges of
 588 attenuation factor t shown in Table 6.2. We contrast this with the permitted range
 589 of t in the case of classical Katz centrality via the dynamic communicability matrix
 590 \mathcal{Q} as defined in (6.1).

591 Figure 6.4 depicts two bar charts which display the normalized centrality values
 592 for both classical and nonbacktracking Katz centralities for $t = 0.5/\rho$ and $t = 0.95/\rho$
 593 respectively, where $1/\rho$ is the upper-limit of the respective regime as given in Table 6.2.
 594 In particular $1/\rho$ is equal to $1/\rho(M)$ (see the proof of [25, Theorem 5.2]) in the case
 595 of nonbacktracking Katz centrality, where M is the matrix described in Definition 5.4
 596 (iv) that is, the form of M in which all forms of backtracking are forbidden. In the
 597 case of classical Katz centrality $1/\rho$ is given by $1/\max_i(\rho(A^{[i]}))$, the reciprocal of the
 598 largest principal eigenvalue of the adjacency matrices. In Figure 6.4 we report results
 599 for 12 nodes, which are selected by taking the union of the 10 most highly ranked
 600 nodes for classical Katz and the 10 most highly ranked nodes for NBT Katz, when
 601 $t = 0.95/\rho$.

602 In Figure 6.5 we plot for the weighted temporal network both the classical and
 603 nonbacktracking Katz centrality values of 10 selected nodes against the attenuation
 604 factor t which ranges from 0% to 99% of its permitted range (as given in Table 6.2).
 605 The 10 nodes were selected such that they are the most central for large values of t .

606 Figure 6.6 presents results for the same experiment, this time carried out with
 607 the binarized version of the temporal network, i.e., the temporal network with all
 608 non-zero weights set to 1.

609 It is interesting to note that nonbacktracking Katz identifies a node distinct from
 610 “Anthony Fauci” as the most central node for large values of t , favouring instead
 611 the node “Jeremy Farrar” which is considerably lower ranked in the static networks
 612 produced from the same data set. Furthermore by comparing Figures 6.5 and 6.6, we
 613 observe the large effect that weighting has on the two centrality measures.

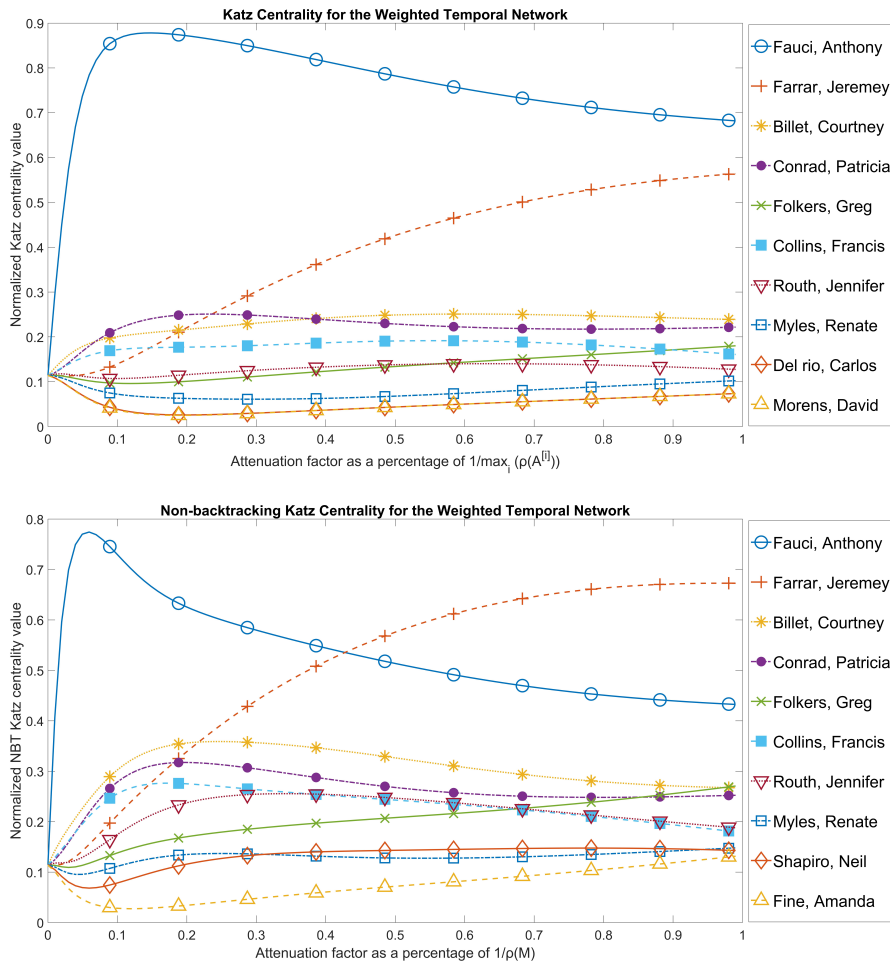


Fig. 6.5: Plots of the normalized Katz (upper) and nonbacktracking Katz (lower) centralities vector values for 10 most prominent nodes (i.e., those with the largest centrality value as of the upper limit of the attenuation factor t) within the weighted temporal network

614 **7. Discussion.** Our aim in this work was to develop a useful theory for the
 615 enumeration of nonbacktracking walks as well as for associated centrality measures,
 616 in the case of edge weights that are combined multiplicatively. We showed in The-
 617 orem 3.1 that in contrast to the unweighted case where a four-term recurrence is
 618 sufficient to count nonbacktracking walks of different lengths, the weighted case gives
 619 rise to a recurrence where the walk count at length k depends on walk counts for all

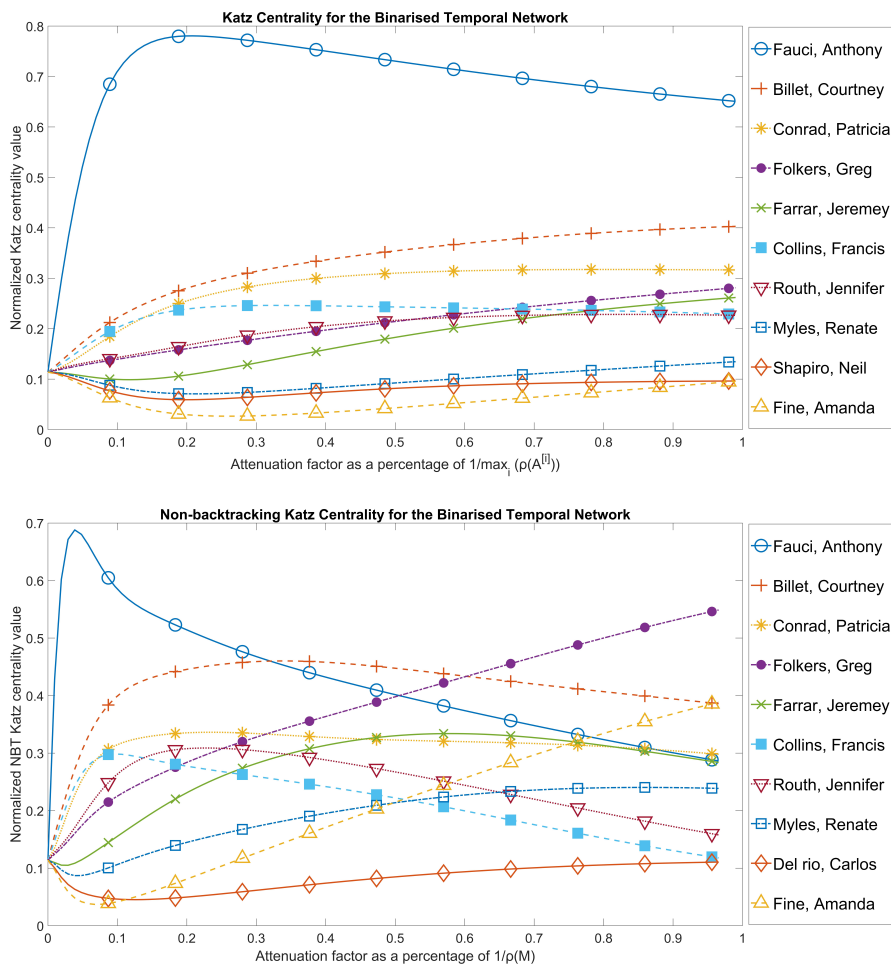


Fig. 6.6: Plots of the normalized Katz (upper) and nonbacktracking Katz (lower) centralities vector values for 10 most prominent nodes (i.e., those with the largest centrality value as of the upper limit of the attenuation factor t) within the binarized temporal network.

620 shorter lengths. Despite this added complexity, the resulting formulas for the stan-
 621 dard generating function in Theorem 3.3 and corresponding node centrality measure
 622 in Corollary 3.4 are straightforward to evaluate.

623 We also showed in Theorem 4.5 that when working at the line graph level, the
 624 introduction of appropriate componentwise square roots allows us to develop a theory
 625 that extends to the unweighted case, with Theorem 4.6 summarizing the results, and
 626 Theorem 5.7 dealing with more general time-evolving graph sequences.

627 A practical take-home message is that a theory of nonbacktracking walk counts
 628 for static or dynamic weighted graphs is available, with corresponding computational
 629 algorithms that have the same complexity as in the unweighted case.

630 **Acknowledgements.** We thank the Editor and the Referees for their useful
631 comments.

632 **References.**

- 633 [1] F. Arrigo, P. Grindrod, D. J. Higham, and V. Noferini. “Non-backtracking walk
634 centrality for directed networks”. In: *Journal of Complex Networks* 6.1 (2018),
635 pp. 54–78.
- 636 [2] F. Arrigo, P. Grindrod, D. J. Higham, and V. Noferini. “On the exponential
637 generating function for non-backtracking walks”. In: *Linear Algebra and Its*
638 *Applications* 79.3 (2018), pp. 781–801.
- 639 [3] F. Arrigo, D. J. Higham, V. Noferini, and R. Wood. “Dynamic Katz and related
640 network measures”. In: *Linear Algebra and its Applications* (2022).
- 641 [4] F. Arrigo, D. J. Higham, and V. Noferini. “Non-backtracking PageRank”. In:
642 *Journal of Scientific Computing* (2019).
- 643 [5] F. Arrigo, D. J. Higham, and V. Noferini. “Beyond non-backtracking: non-
644 cycling network centrality measures”. In: *Proc. R. Soc. A* 476.2235 (2020),
645 p. 20190653.
- 646 [6] A. R. Benson, N. Veldt, and D. F. Gleich. *fauci-email: a json digest of Anthony*
647 *Fauci’s released emails*. 2021. arXiv: [2108.01239](https://arxiv.org/abs/2108.01239) [cs.SI].
- 648 [7] M. Benzi and C. Klymko. “Total communicability as a centrality measure”. In:
649 *Journal of Complex Networks* 1.2 (2013), pp. 124–149.
- 650 [8] N. Bettendorf and J. Leopold. *Anthony Fauci’s Emails Reveal The Pressure*
651 *That Fell On One Man*. June 2021. URL: [https://s3.documentcloud.org/](https://s3.documentcloud.org/documents/20793561/leopold-nih-foia-anthony-fauci-emails.pdf)
652 [documents/20793561/leopold-nih-foia-anthony-fauci-emails.pdf](https://s3.documentcloud.org/documents/20793561/leopold-nih-foia-anthony-fauci-emails.pdf).
- 653 [9] S. Bhadra and A. Ferreira. “Complexity of connected components in evolving
654 graphs and the computation of multicast trees in dynamic networks”. In: *Inter-*
655 *national Conference on Ad-Hoc Networks and Wireless*. Springer. 2003, pp. 259–
656 270.
- 657 [10] R. Bowen and O. E. Lanford. “Zeta functions of restrictions of the shift trans-
658 formation”. In: *Global Analysis: Proceedings of the Symposium in Pure Mathe-*
659 *matics of the Americal Mathematical Society, University of California, Berkely,*
660 *1968*. Ed. by S.-S. Chern and S. Smale. American Mathematical Society, 1970,
661 pp. 43–49.
- 662 [11] E. Estrada. *The Structure of Complex Networks*. Oxford: Oxford University
663 Press, 2011.
- 664 [12] E. Estrada and J. A. Rodríguez-Velázquez. “Subgraph centrality in complex
665 networks”. In: *Physical Review E* 71 (2005), p. 056103.
- 666 [13] C. Fenu and D. J. Higham. “Block matrix formulations for evolving networks”.
667 In: *SIAM Journal on Matrix Analysis and Applications* 38.2 (2017), pp. 343–
668 360.
- 669 [14] P. Grindrod, D. J. Higham, and V. Noferini. “The deformed graph Laplacian
670 and its applications to network centrality analysis”. In: *SIAM Journal on Matrix*
671 *Analysis and Applications* 39.1 (2018), pp. 310–341.
- 672 [15] P. Grindrod, M. C. Parsons, D. J. Higham, and E. Estrada. “Communicability
673 across evolving networks”. In: *Physical Review E* 83.4 (2011), p. 046120.
- 674 [16] K. Hashimoto. “On Zeta and L-functions of finite graphs”. In: *Intl. J. Math.* 1
675 (1990), pp. 381–396.
- 676 [17] P. Holme and J. Saramäki. “Temporal Networks”. In: *Physics Reports* 519
677 (2012), pp. 97–125.

- 678 [18] M. D. Horton, H. M. Stark, and A. A. Terras. “What are zeta functions of graphs
679 and what are they good for?” In: *Quantum graphs and their applications*. Ed. by
680 G. Berkolaiko, R. Carlson, S. A. Fulling, and P. Kuchment. Vol. 415. Contemp.
681 Math. 2006, pp. 173–190.
- 682 [19] L. Katz. “A new index derived from sociometric data analysis”. In: *Psychome-
683 trika* 18 (1953), pp. 39–43.
- 684 [20] M. Kempton. “Non-Backtracking Random Walks and a Weighted Ihara’s The-
685 orem,” in: *Open J. Discrete Math.* 6 (2016), pp. 207–226.
- 686 [21] T. Komatsu, N. Konno, and I. Sato. “A zeta function with respect to non-
687 backtracking alternating walks for a digraph”. In: *Linear Algebra and its Appli-
688 cations* 620 (2021), pp. 344–367.
- 689 [22] H. Mizuno and I. Sato. “Zeta functions of digraphs”. In: *Linear Algebra and its
690 Applications* 336.1–3 (2001), pp. 181–190.
- 691 [23] P. Mucha, T. Richardson, K. Macon, M. Porter, and J. Onnela. “Community
692 structure in time-dependent, multiscale, and multiplex networks”. In: *Science*
693 328 (2010), pp. 876–878.
- 694 [24] M. E. J. Newman. *Networks: an Introduction*. Oxford: Oxford University Press,
695 2010.
- 696 [25] V. Noferini and M. C. Quintana. *Generating functions of non-backtracking walks
697 on weighted digraphs: radius of convergence and Ihara’s theorem*. 2023. arXiv:
698 <https://arxiv.org/pdf/2307.14200.pdf> [math.CO].
- 699 [26] H. Stark and A. Terras. “Zeta functions of finite graphs and coverings”. In:
700 *Advances in Mathematics* 121.1 (1996), pp. 124–165.
- 701 [27] A. Tarfulea and R. Perlis. “An Ihara formula for partially directed graphs”. In:
702 *Linear Algebra and its Applications* 431 (2009), pp. 73–85.
- 703 [28] G. Timár, R. A. da Costa, S. N. Dorogovtsev, and J. F. F. Mendes. “Approx-
704 imating nonbacktracking centrality and localization phenomena in large net-
705 works”. In: *Phys. Rev. E* 104 (2021), p. 054306.
- 706 [29] L. Torres, K. S. Chan, H. Tong, and T. Eliassi-Rad. “Nonbacktracking eigen-
707 values under node removal: X-centrality and targeted immunization”. In: *SIAM
708 Journal on Mathematics of Data Science* 3 (2021).
- 709 [30] L. Torres, P. Suarez-Serrato, and T. Eliassi-Rad. “Non-backtracking cycles:
710 Length spectrum theory and graph mining applications”. In: *Journal of Ap-
711 plied Network Science* 41 (2019).
- 712 [31] P. Van Doreen and C. Fraikin. “Similarity matrices for colored graphs”. In: *Bull.
713 Belg. Math. Soc. Simon Stevin* 16 (2009), pp. 705–722.